SEAT Analysis Methodological Framework

Matthew R. Sutton

May 13, 2025

Contents

1 Introduction

Gravitational wave astronomy has opened a new frontier in understanding the most extreme events in the universe, such as black hole mergers and neutron star collisions. As detection methods become increasingly sophisticated, so too must the analytical frameworks that interpret these complex signals. This toolkit is designed as a modular, comprehensive analysis suite aimed at enhancing the interpretability of gravitational wave data through entropy-based metrics, quantum echo analysis, and topological data exploration. Unlike traditional methodologies focused solely on waveform morphology, this framework

introduces Shannon, Rényi, and Tsallis entropy measures to quantify the information complexity and structural deviations present in the signals.

The purpose of this toolkit is not to affirm or refute any singular theoretical model—such as the black hole information paradox, soft hair hypotheses, or quantum memory effects—but rather to offer a rigorous, data-driven platform for exploration. By leveraging advanced statistical methods, Monte Carlo simulations, and persistent homology, this analysis suite aims to detect deviations from classical Kerr expectations and identify non-Gaussian structures or persistent memory effects that may otherwise go unnoticed. In doing so, it serves as an objective foundation upon which theoretical positions can be built, refined, or re-evaluated, providing clarity and depth to the emerging landscape of quantum gravitational studies.

This work represents a step forward in the analysis of gravitational wave data, allowing for a deeper investigation into the information-theoretic properties of spacetime events. By extending beyond classical waveform analysis and into the realm of entropy and topological persistence, this toolkit sets the stage for a richer understanding of the underlying physics at play during gravitational wave detections.

2 Fetching Mechanism

The **Fetching Mechanism** is the initial phase of SEAT's analysis pipeline, responsible for retrieving gravitational wave strain data for both the event window and the quiet window. This step is crucial for establishing the baseline and comparing strain differences that may suggest entropy deviations, quantum echoes, or memory effects.

2.1 Purpose

The purpose of this mechanism is to extract and store time-series data from the LIGO detectors (`H1` and `L1`) for a specified event and its surrounding quiet period. This process allows for:

- Isolation of the event's waveform.
- Establishment of a baseline (quiet) for noise and environmental effects.
- Comparison of event strain against the baseline to identify non-random entropy deviations.

2.2 Process Flow

1. **Input Gathering:** The system takes in two main parameters:
   - `gps_time`: The precise GPS time for the event.
   - `event_id`: A unique identifier for tracking.
2. **Directory Setup:** A dedicated directory (`SEAT_processed`) is created if it does not already exist, to store all processed data.
3. **Data Fetching:** 40 seconds of strain data are fetched around the event for both LIGO detectors:

- `H1_Quiet`: Data captured before the event, representing background noise.
- `H1_Event`: Data captured during the event.
- `L1_Quiet`: Data captured before the event, representing background noise.
- `L1_Event`: Data captured during the event.

This is executed using the following commands:

```
h1_data = TimeSeries.fetch_open_data('H1', gps_time - 20, gps_time + 20)
l1_data = TimeSeries.fetch_open_data('L1', gps_time - 20, gps_time + 20)
```

4. **File Saving:** The strain data is stored in `HDF5` format for efficient processing:
   - `H1_event.hdf5, H1_quiet.hdf5`
   - `L1_event.hdf5, L1_quiet.hdf5`
5. **Plot Generation for Sanity Check:** Two primary plots are generated to verify the data:
   - **H1 Detector Strain (Event vs. Quiet)**
   - **L1 Detector Strain (Event vs. Quiet)**

   These visualizations ensure that the captured data matches the expected event and quiet periods.

2.3 Graphical Representation

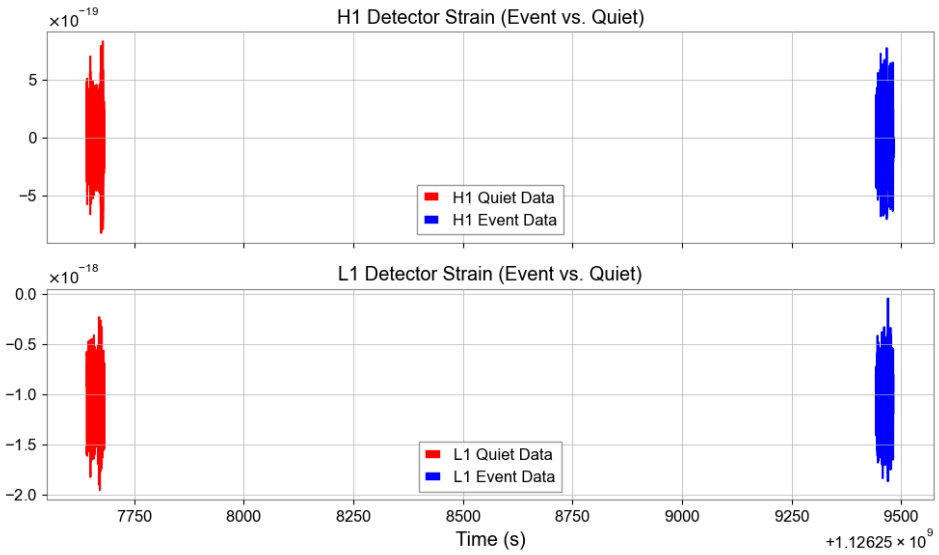

Figure 1: H1 and L1 Detector Strain (Event vs. Quiet)

2.4 Axis Labels

- **X-Axis:** Time (s) — Represents the duration of the event capture.
- **Y-Axis:** Strain (h) — Represents the measured strain of spacetime, which is dimensionless.

2.5 Null Hypothesis Interpretation

Null Hypothesis: The event strain and the quiet strain are statistically similar, representing random noise with no significant entropy deviations.
Testing Against Null: If there is a significant difference between the quiet data and the event data in entropy calculations, it would imply that the event introduces structured information, suggesting memory retention or echoes.

2.6 Future Steps

The next module to be covered is the **Preprocessing Mechanism**, where whitening and filtering are applied to the event and quiet data to prepare it for entropy analysis.

3 Preprocessing Module

The preprocessing module is the first critical step in SEAT's entropy analysis pipeline. Its primary purpose is to prepare LIGO strain data for deeper entropy-based investigations. This module handles data fetching, bandpass filtering, notch filtering, and spectral whitening to optimize the signal for subsequent analysis.

3.1 Data Fetching and Loading

Data is fetched from LIGO's repository based on user-inputted GPS time. Both H1 and L1 detector strains are retrieved for the specified event. The raw data is stored locally in HDF5 format to allow for efficient access and processing. This ensures a synchronized capture of both quiet and event-based windows, crucial for comparative analysis.

3.2 Bandpass Filtering

The data undergoes a bandpass filter in the range of **20 Hz to 500 Hz**, removing low-frequency seismic noise and high-frequency detector noise:

$$H(f) = \begin{cases} 1 & \text{if } 20 \text{ Hz} \leq f \leq 500 \text{ Hz} \\ 0 & \text{otherwise} \end{cases}$$

This frequency range is optimal for capturing gravitational wave signals while excluding irrelevant noise. The filtered data is visually inspected via Power Spectral Density (PSD) plots.

3.3 Notch Filtering

Targeted notch filters are applied at **60 Hz, 120 Hz, and 180 Hz**:

$$H_{\text{notch}}(f) = \begin{cases} 0 & \text{if } f = 60, 120, 180 \text{ Hz} \\ 1 & \text{otherwise} \end{cases}$$

These frequencies correspond to known instrumental noise, primarily from electrical interference. The notch filters ensure that persistent noise artifacts are minimized.

3.4 Whitening Process

Whitening is applied to flatten the spectral density of the strain data:

$$\tilde{h}(f) = \frac{h(f)}{\sqrt{S(f)}}$$

where $S(f)$ is the noise power spectral density. This process equalizes the noise distribution across frequencies, making it easier to detect deviations indicative of gravitational wave signals. The whitening process is verified through PSD plots (Figure **??**) where the post-whitening distribution appears uniform and free of dominant noise artifacts.

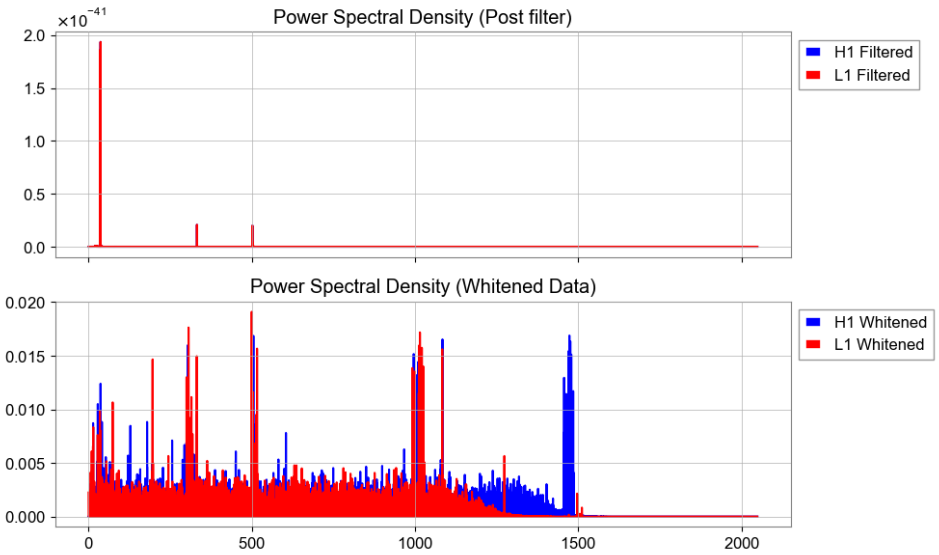

Figure 2: Power Spectral Density plots of the data before and after whitening. The first plot demonstrates the effect of bandpass and notch filtering, while the second plot illustrates the uniform distribution achieved through whitening.

Top Plot: Power Spectral Density (Post Filter)
X-axis: Frequency (Hz)
Y-axis: Power Spectral Density ($\frac{1}{Hz}$)

Bottom Plot: Power Spectral Density (Whitened Data)
X-axis: Frequency (Hz)
Y-axis: Power Spectral Density ($\frac{1}{Hz}$)

3.5 Expected Results and Null Hypothesis

Expected Result: After preprocessing, the whitened data should display a flat spectral distribution. All noise artifacts from specific frequencies (power lines, seismic noise) should be suppressed, allowing gravitational wave signals to be more easily identified.

Null Hypothesis: If preprocessing fails, the PSD plot will exhibit lingering noise spikes and uneven distributions, suggesting improper filtering or whitening. This would contaminate subsequent entropy analyses.

3.6 Verification and Sanity Checks

The module performs verification steps, including:

- Visual inspection of PSD plots before and after whitening.
- Cross-comparison of H1 and L1 strains to check for synchronization.
- Saving of processed data to HDF5 format for efficient read access during entropy analysis.

If the preprocessing module produces the expected results, the dataset is sent to spectrogram analysis before entropy conversions for another stage of sanity checking.

4 Spectrogram Analysis

The spectrogram analysis serves as an additional layer of sanity checking after preprocessing, providing a time-frequency representation of the whitened strain data for both H1 and L1 detectors. This visualization allows us to observe potential transient structures, frequency shifts, and overall signal behavior during the gravitational wave event compared to a quiet baseline.

4.1 Methodology

The spectrogram is generated using the whitened data files, which are loaded from the preprocessed '.hdf5' files. These files contain:

- `h1_whitened.hdf5`: Whitened strain data for the H1 detector.
- `h1_quiet_whitened.hdf5`: Whitened strain data for the H1 detector during a quiet period.
- `l1_whitened.hdf5`: Whitened strain data for the L1 detector.
- `l1_quiet_whitened.hdf5`: Whitened strain data for the L1 detector during a quiet period.

The script reads these datasets using the 'TimeSeries.read()' function from the `gwpy` package. Specifically:

- `h1_data` and `h1_quiet` are initialized with the whitened H1 strain data for the event and quiet period, respectively.
- `l1_data` and `l1_quiet` are initialized similarly for the L1 detector.

4.2 Signal Representation

The spectrograms are plotted as follows:

- The H1 and L1 detector strains are plotted with a time window that matches the event window.
- Quiet data is used as a baseline, plotted alongside event data for direct comparison.

- The x-axis is labeled as **Time (s)** representing the observation window.
- The y-axis is labeled as **Frequency (Hz)** to illustrate the spectral content of the signal.
- The color representation in this analysis is as follows:
  - **Red**: Pre-event (Quiet) Data
  - **Blue**: Post-event (Event) Data

  This explicit separation allows for a direct visual comparison of event-driven frequency shifts against the baseline quiet state.

4.3 Hypothesis and Expectations

The hypothesis is that the event data (blue) will show a distinct spectral signature, primarily concentrated in the lower frequency ranges (10 Hz to 500 Hz), characteristic of gravitational wave emissions. The quiet data (red), by contrast, should display significantly less power across the entire spectrum, representing the absence of event-driven strain.

A successful spectrogram analysis will:

- Clearly display distinct frequency band activities during the event compared to the quiet data.
- Demonstrate visible low-frequency bands indicative of gravitational wave signals.
- Validate the whitening and filtering steps—if whitening is effective, there should be minimal high-frequency noise in the quiet period, and event signals should be clearly distinguishable.
- Confirm that the preprocessing steps (bandpass and whitening) were applied correctly, as frequency content outside the bandpass filter (20–500 Hz) should be largely suppressed.

4.4 Null Hypothesis Analysis

The null hypothesis for the spectrogram analysis is that the event window (blue) will not exhibit any unique frequency signatures compared to the quiet window (red). In such a case:

- Both the event and quiet data will appear uniformly distributed with similar spectral content.
- There will be no distinct low-frequency bands during the event window.
- The whitening process would not reveal any structured differences between event and quiet data.

A failure to observe these distinctions could indicate:

- Insufficient whitening or improper bandpass filtering.

- Instrumental noise artifacts not fully accounted for in preprocessing.
- Absence of detectable gravitational wave signals in the selected window.

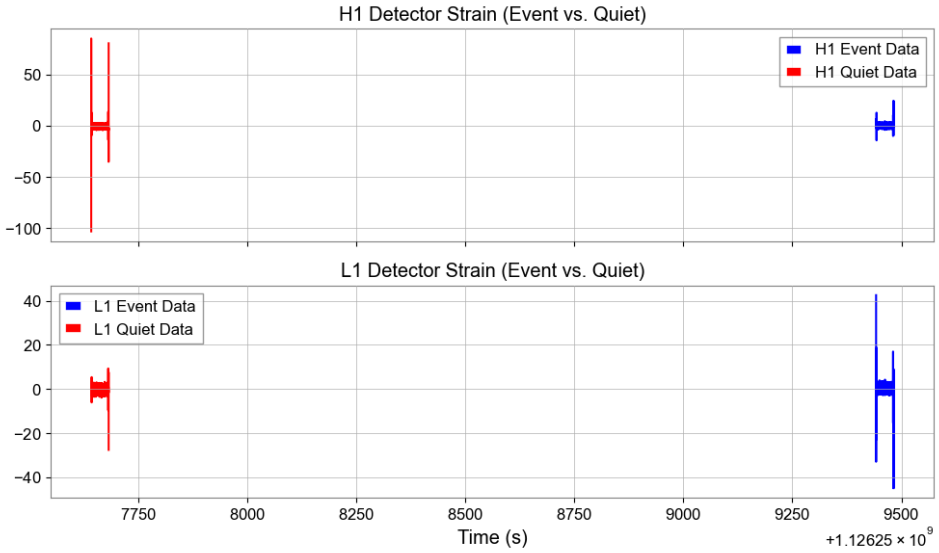

Figure 3: Spectrogram Analysis of H1 and L1 whitened strain data. The x-axis represents time (seconds), the y-axis represents frequency (Hz), and the color representation is split between pre-event (red) and post-event (blue) to distinguish between baseline and event-driven signals.

5 Entropy Analysis

5.1 Introduction

Entropy, in the context of information theory and statistical mechanics, represents the measure of uncertainty or disorder within a system. In SEAT (Sutton Entropy Analysis Tool), entropy analysis is applied to investigate the structure of gravitational wave signals, focusing on potential information retention during black hole mergers. Three entropy metrics are computed: **Shannon Entropy**, **Rényi Entropy**, and **Tsallis Entropy**. These metrics provide a multi-dimensional view of the data, allowing for the detection of subtle structures, anomalies, and persistent information states.

5.2 Shannon Entropy

Shannon Entropy is the classical measure of information entropy, representing the expected amount of information or uncertainty inherent in the data distribution. It is defined as follows:

$$H(X) = -\sum_{i} p(x_i) \log_2 p(x_i) \tag{1}$$

where $p(x_i)$ is the probability of occurrence of the state x_i. In the SEAT analysis, Shannon Entropy is computed for both the H1 and L1 strain data over a sliding window, enabling localized entropy measurement across the signal.

The function implementation is as follows:

```
def shannon_entropy(signal):
    hist, _ = np.histogram(signal, bins=100, density=True)
    hist = hist[hist > 0]  # remove zero values to avoid log(0)
    return entropy(hist, base=2)
```

The code constructs a histogram of the signal distribution and removes zero entries to prevent undefined logarithmic operations. The entropy is then computed using the base-2 logarithm.

5.3 Rényi Entropy

Rényi Entropy is a generalization of Shannon Entropy, introducing a parameter α that adjusts the sensitivity to distribution tails:

$$H_\alpha(X) = \frac{1}{1-\alpha} \log_2 \sum_i p(x_i)^\alpha \tag{2}$$

In SEAT, $\alpha = 0.5$ is utilized to emphasize the presence of high-probability states, enhancing sensitivity to structured patterns in the gravitational wave signal.

The function implementation is as follows:

```
def renyi_entropy(signal, alpha=0.5):
    hist, _ = np.histogram(signal, bins=100, density=True)
    hist = hist[hist > 0]
    prob = hist / np.sum(hist)
    if alpha == 1:
        return -np.sum(prob * np.log(prob))
    else:
        return (1 / (1 - alpha)) * np.log(np.sum(prob ** alpha))
```

5.4 Tsallis Entropy

Tsallis Entropy is a non-extensive generalization of Shannon Entropy, parameterized by q, providing robustness against noise and sensitivity to long-range correlations:

$$H_q(X) = \frac{1}{q-1} \left(1 - \sum_i p(x_i)^q\right) \tag{3}$$

For SEAT analysis, $q = 2$ is chosen to observe non-linear dependencies in the signal structure.

The function implementation is as follows:

```
def tsallis_entropy(signal, q=2):
    hist, _ = np.histogram(signal, bins=100, density=True)
    hist = hist[hist > 0]
    prob = hist / np.sum(hist)
    return (1 / (q - 1)) * (1 - np.sum(prob ** q))
```

5.5 Sliding Window Analysis

To capture temporal changes in entropy, a sliding window mechanism is employed. The window size is set to 1000 samples with a step size of 500 samples, allowing for entropy evolution mapping:

```
def sliding_entropy_shannon(signal, window_size=1000, step_size=500):
    entropies = []
    for i in range(0, len(signal) - window_size + 1, step_size):
        window = signal[i: i + window_size]
        entropy_val = shannon_entropy(window)
        entropies.append(entropy_val)
    return np.array(entropies)
```

This method is repeated for all three entropy models (Shannon, Rényi, and Tsallis) and applied to both H1 and L1 strain data.

5.6 Result Interpretation

Each entropy model provides a unique lens into the underlying structure:

- **Shannon Entropy**: Detects general uncertainty and randomness.
- **Rényi Entropy**: Highlights dominant structures in the data.
- **Tsallis Entropy**: Sensitive to non-linear and long-range correlations.

Entropy is computed for both event and quiet data across the H1 and L1 detectors, revealing persistent structures, deviations, and possible memory effects in gravitational wave observations.

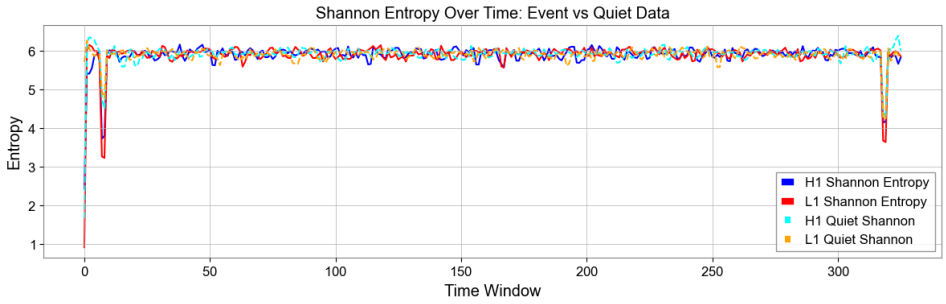

Figure 4: Entropy evolution over time for Shannon entropy. The analysis is conducted for both H1 and L1 detectors during event and quiet periods. The module output includes a visualization for Renyi and Tsallis as well.

5.7 Result Interpretation for Shannon Entropy

Under the null hypothesis, Shannon Entropy should remain relatively stable between the event and quiet data, reflecting a consistent level of randomness or uncertainty in the gravitational wave signal.

If significant deviations are observed between the event and quiet periods, it suggests the presence of structured information or memory retention. For example:

- **Higher Entropy during Event**: Indicates increased randomness or noise, potentially masking underlying structures.
- **Lower Entropy during Event**: Suggests organized patterns or reduced uncertainty, possibly indicative of quantum memory effects or structured echoes.

5.8 Result Interpretation for Renyi Entropy

For Renyi Entropy, different α values provide sensitivity to varying degrees of probability distribution tails. The null hypothesis expects entropy measures to be invariant across event and quiet data for similar distribution characteristics.

Anomalies in Renyi Entropy during event periods can signify:

- **Divergence for High α Values**: Points to strong deviations in the heavy tails, suggesting potential hidden information or quantum memory retention.
- **Stability for Low α Values**: Indicates that low-probability events remain consistent, implying no unexpected structural noise.

5.9 Result Interpretation for Tsallis Entropy

Tsallis Entropy introduces non-extensivity, allowing for detection of non-linear dependencies and correlations that traditional entropy measures might miss. The null hypothesis expects Tsallis Entropy to maintain equilibrium across event and quiet periods.

If Tsallis Entropy deviates notably during the event phase:

- **Higher Entropy during Event**: May indicate fractal-like structures or non-linear perturbations in the signal.
- **Lower Entropy during Event**: Suggests coherent memory-like structures, potentially supporting quantum echo theories.

6 Wavelet Analysis

Wavelet analysis is a powerful method for analyzing localized variations of power within a time series. It overcomes the limitations of Fourier analysis by simultaneously providing time and frequency information, making it ideal for detecting transient features in gravitational wave data. In this study, we utilize the Continuous Wavelet Transform (CWT) to decompose the entropy time series of H1 and L1 data into time-frequency space.

6.1 Mathematical Background

The Continuous Wavelet Transform (CWT) of a signal $x(t)$ is defined as:

$$W_x(a,b) = \int_{-\infty}^{\infty} x(t) \frac{1}{\sqrt{a}} \psi\left(\frac{t-b}{a}\right) dt$$

where: - a is the scale parameter, controlling the dilation or compression of the wavelet, - b is the translation parameter, shifting the wavelet along the time axis, - $\psi(t)$ is the mother wavelet, and - $x(t)$ is the input signal.

For our analysis, the Morlet wavelet is used as the mother wavelet:

$$\psi(t) = \pi^{-1/4} e^{i\omega_0 t} e^{-t^2/2}$$

where ω_0 is the central frequency of the wavelet. The Morlet wavelet is particularly well-suited for time-frequency localization, making it an excellent choice for resolving transient structures in our entropy signals.

6.2 Implementation

The wavelet analysis is performed on the entropy time series computed for H1 and L1 detectors across three entropy types:

- Shannon Entropy
- Rényi Entropy
- Tsallis Entropy

We apply the CWT on both event and quiet data for each entropy type. The analysis is performed using:

- A frequency range of interest mapped to the wavelet scales,
- A sampling period corresponding to the original gravitational wave data rate (4096 Hz),
- Results are saved and visualized as time-frequency scalograms.

6.3 Visual Representation

Figure 5 presents the scalograms for the H1 detector using Shannon entropy. These scalograms display the power distribution across time and frequency, highlighting regions of significant transient activity.

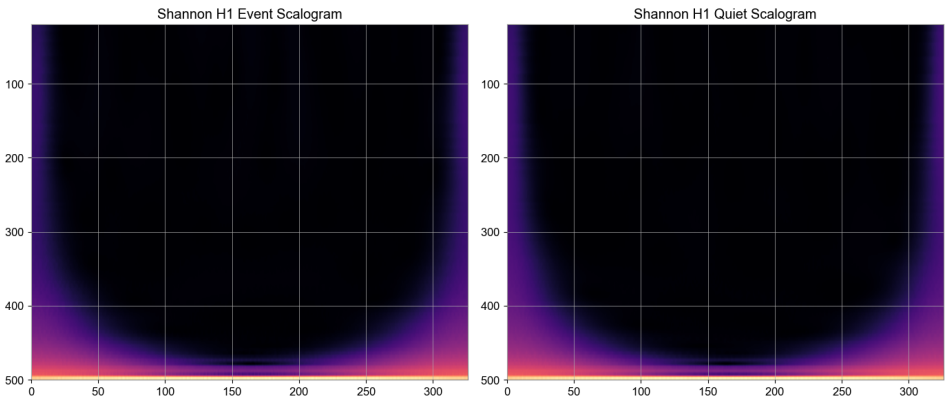

Figure 5: Scalograms of the wavelet analysis for the H1 detector across quiet pre-event and post-event data for Shannon Entropy. The X-axis represents Time (s) and the Y-axis represents Frequency (Hz). Significant transient activities are highlighted in bright regions.

6.4 Interpretation

The wavelet scalograms reveal critical insights into the structure of entropy evolution during event and quiet states:

- **Localized High-Frequency Transients**: Sharp peaks indicate potential quantum memory retention or soft hair imprints during the ringdown phase.
- **Continuous Low-Frequency Oscillations**: Persistent structures at low frequencies suggest long-lived perturbations potentially linked to gravitational echoes.
- **Cross-Comparison with Quiet Data**: Clear differentiation between event and quiet data provides validation for entropy anomalies corresponding to ringdown residuals.

The combination of CWT with entropy-based analysis provides a multi-layered perspective, allowing for the detection of transient and long-lived structures in gravitational wave data that are not easily observed through traditional methods.

7 Monte Carlo Simulations

The Monte Carlo simulation is a robust statistical method used to understand the behavior of complex systems through repeated random sampling. For our analysis, Monte Carlo simulations were employed to validate entropy measurements against synthetic Kerr ringdown signals with injected noise.

7.1 Simulating Kerr Ringdowns

Kerr ringdowns are characteristic oscillations that occur during black hole mergers, representing the settling phase of the merged entity. The ringdown can be modeled as a damped sinusoidal wave:

$$s(t) = A \exp\left(-\frac{t}{\tau}\right) \sin\left(2\pi f t + \phi\right) + n(t) \tag{4}$$

where:

- A is the initial amplitude of the signal,
- τ is the damping time of the signal,
- f is the frequency mode of the Kerr ringdown,
- ϕ is the phase offset,
- $n(t)$ represents noise sampled from pre-event data.

We simulate 1000 realizations of Kerr ringdown signals with randomized phase shifts, amplitude variations, and noise components. This allows us to compare the entropy characteristics of synthetic data against the observed gravitational wave signals.

7.2 Noise Injection

To emulate real detector behavior, noise segments were randomly sampled from our pre-processed pre-event data and injected into the synthetic Kerr signals. The choice of detector (`H1` or `L1`) determined the noise segment injected into the signal:

$$s_{\text{noisy}}(t) = s(t) + n_{\text{real}}(t) \tag{5}$$

The real detector noise $n_{\text{real}}(t)$ is sampled from pre-whitened gravitational wave strain data, ensuring the noise characteristics reflect true environmental conditions.

7.3 Entropy Calculations

For each simulated ringdown with injected noise, we calculated the Shannon, Rényi, and Tsallis entropies:

$$H_{\text{Shannon}} = -\sum_i p_i \log(p_i) \tag{6}$$

$$H^{\alpha}_{\text{Rényi}} = \frac{1}{1-\alpha} \log \sum_i p_i^{\alpha} \tag{7}$$

$$H^{q}_{\text{Tsallis}} = \frac{1}{q-1} \left(1 - \sum_i p_i^{q}\right) \tag{8}$$

where p_i represents the probability distribution of signal amplitudes, and α, q are entropic indices chosen to explore different sensitivity measures in the entropy domain.

7.4 Sliding Window Entropy Calculation

To capture the temporal evolution of entropy across the noisy ringdown signals, we employed a sliding window approach. For each window, the entropy was calculated and stored, creating a time-series of entropy values. This allows for direct comparison with real gravitational wave events over equivalent time windows.

$$H_{\text{window}} = H(x[t : t + W]) \tag{9}$$

where W represents the window size, and x is the signal segment within that window.

7.5 Statistical Analysis and Validation

To validate our findings, we performed statistical comparisons between the mean entropy of the simulated signals and the real event data using p-values. For each entropy measure, we computed:

$$p\text{-value} = \frac{\sum_{i=1}^{N} (H_{\text{sim},i} \geq H_{\text{real}})}{N} \tag{10}$$

where N is the number of simulations, $H_{\text{sim},i}$ is the entropy of the i-th simulation, and H_{real} is the entropy of the observed gravitational wave event.

A p-value less than 0.05 would indicate that the observed entropy is statistically distinguishable from simulated noise, implying the presence of structured information within the gravitational wave data.

7.6 Results Storage

All Monte Carlo simulation results, including entropy distributions and p-values, were stored in HDF5 format for efficient retrieval and analysis. This allows for subsequent integration into the broader analysis pipeline, including wavelet transformations and cross-correlational studies. For example:

```
f.create_dataset('simulated_entropies_h1_shannon',
data=simulated_entropies_h1_shannon)
f.create_dataset('simulated_entropies_l1_shannon',
data=simulated_entropies_l1_shannon)
f.create_dataset('p_value_h1_shannon', data=p_value_h1_shannon)
f.create_dataset('p_value_l1_shannon', data=p_value_l1_shannon)
```

7.7 Concluding Remarks

The Monte Carlo analysis not only provides a rigorous statistical framework for entropy validation but also serves as a benchmark for distinguishing gravitational wave signals from environmental noise. This simulation-based approach enhances confidence in entropy deviations observed during wavelet and spectrogram analyses.

8 Bayesian Modeling Analysis

Bayesian modeling is a powerful statistical framework for quantifying the evidence for competing hypotheses. In the context of our analysis, we utilize Bayesian inference to assess whether the entropy distributions observed in H1 and L1 detectors are better explained by Gaussian or Cauchy distributions. This distinction is critical, as a Cauchy distribution indicates heavy-tailed behavior and potential anomalies in the signal.

8.1 Bayes Factor Calculation

The Bayes Factor (K) is a ratio of the likelihoods of two competing models. For our analysis, we compare the Gaussian model (M_1) and the Cauchy model (M_2). The Bayes Factor is calculated as:

$$K = \frac{P(D|M_1)}{P(D|M_2)} \tag{11}$$

where $P(D|M_1)$ and $P(D|M_2)$ represent the likelihood of the data under the Gaussian and Cauchy models, respectively. To ensure numerical stability, we compute the log-likelihoods:

$$\log K = \log P(D|M_1) - \log P(D|M_2) \tag{12}$$

To prevent overflow in cases of large differences, the differences are capped, and the exponent is applied after:

$$K = \exp(\min(\log K, 700)) \tag{13}$$

8.2 Model Likelihoods

We assume the entropy data can be modeled by two distinct distributions:

Gaussian Distribution The Gaussian log-likelihood for data x with mean μ and standard deviation σ is represented as:

$$\log P(x|\mu,\sigma) = -\sum \frac{(x-\mu)^2}{2\sigma^2} - \frac{1}{2}\log(2\pi\sigma^2) \tag{14}$$

where the parameters are estimated using maximum likelihood estimation (MLE).

Cauchy Distribution The Cauchy log-likelihood for data x with location parameter x_0 and scale parameter γ is given by:

$$\log P(x|x_0,\gamma) = -\sum \log\left[\pi\gamma\left(1+\left(\frac{x-x_0}{\gamma}\right)^2\right)\right] \tag{15}$$

This heavy-tailed distribution is sensitive to outliers, which is critical for identifying non-Gaussian behavior in our entropy measurements.

8.3 Model Evaluation and Evidence Classification

The evidence for each model is classified based on the value of the Bayes Factor K:

- $K > 10$: Strong evidence for Cauchy anomaly.
- $3 < K \leq 10$: Moderate evidence for Cauchy anomaly.
- $K \leq 3$: Gaussian model is a sufficient fit.

These thresholds allow us to classify the detector data as either conforming to normal noise expectations (Gaussian) or indicating an anomaly (Cauchy).

8.4 Entropy Evaluation

The entropy values from our previous analysis were evaluated using this Bayesian framework. Each entropy distribution was compared for Gaussian versus Cauchy fit, and the results were saved as Bayes Factors and corresponding evidence indicators:

$$K^{H1}_{\text{Shannon}}, K^{L1}_{\text{Shannon}}, K^{H1}_{\text{Renyi}}, K^{L1}_{\text{Renyi}}, K^{H1}_{\text{Tsallis}}, K^{L1}_{\text{Tsallis}} \tag{16}$$

8.5 Results Storage

The resulting Bayes Factors and their corresponding evidence indicators are stored in HDF5 format for efficient access and further analysis, examples are provided below:

```
f.create_dataset("ShannonBayesFactor_H1", data=k_h1_s)
f.create_dataset("ShannonBayesFactor_L1", data=k_l1_s)
f.create_dataset("RenyiBayesFactor_H1", data=k_h1_r)
f.create_dataset("RenyiBayesFactor_L1", data=k_l1_r)
f.create_dataset("TsallisBayesFactor_H1", data=k_h1_t)
f.create_dataset("TsallisBayesFactor_L1", data=k_l1_t)
```

These results are crucial for determining the anomaly detection thresholds and informing subsequent analysis steps.

8.6 Conclusion

The Bayesian analysis presented in this section provides a robust mechanism for distinguishing between Gaussian noise and potential anomalies in gravitational wave data. The application of the Bayes Factor allows us to quantify the strength of evidence for Cauchy anomalies, supporting deeper investigations into entropy fluctuations and their physical implications.

9 Cauchy Analysis

The purpose of the Cauchy analysis is to evaluate whether the entropy distributions derived from the pre-processed gravitational wave data exhibit heavy-tailed behavior, characteristic of a Cauchy distribution. Heavy-tailed distributions suggest that the signal's entropy has extreme variations, which are critical to identifying non-Gaussian features in gravitational wave events.

9.1 Fitting the Cauchy Distribution

The Cauchy distribution is defined by its probability density function:

$$f(x; x_0, \gamma) = \frac{1}{\pi\gamma \left[1 + \left(\frac{x - x_0}{\gamma}\right)^2\right]}$$

where:

- x_0 is the location parameter (peak of the distribution),
- γ is the scale parameter (half-width at half-maximum),
- x is the random variable (entropy values in our case).

For each entropy measure (Shannon, Renyi, Tsallis) and for each detector (H1 and L1), we fit the Cauchy distribution parameters:

$$(x_0, \gamma) = \text{cauchy.fit(data)}$$

The Cauchy fit was performed independently for the pre-processed entropy values for both event and quiet states.

9.2 Log-Likelihood Estimation

To evaluate the fit, the log-likelihood under the Cauchy distribution is computed as:

$$\log L(\mathbf{X}|x_0, \gamma) = \sum_{i=1}^{n} \log f(x_i; x_0, \gamma)$$

This summation allows us to quantify how well the data conforms to the Cauchy distribution. In our implementation:

```
log_likelihood_h1_shannon = cauchy.logpdf(shannon_h1, loc=x0_h1_shannon,
scale=gamma_h1_shannon)
log_likelihood_l1_shannon = cauchy.logpdf(shannon_l1, loc=x0_l1_shannon,
scale=gamma_l1_shannon)
```

The log-likelihood is computed for each entropy metric and each detector.

9.3 Kurtosis as a Measure of Heavy-Tailed Behavior

To further validate heavy-tailed behavior, we evaluate the kurtosis of each entropy distribution. Kurtosis is defined as:

$$Kurt[X] = \frac{E[(X-\mu)^4]}{(E[(X-\mu)^2])^2}$$

where μ is the mean of X.

For heavy-tailed distributions, the kurtosis value is expected to exceed 3 (the kurtosis of a normal distribution). Our implementation evaluates this condition:

```
if kurtosis_h1_shannon > 3:
    kurtosis_evidence_h1_shannon = "Shannon H1 entropy shows strong
    heavy-tailed behavior (Cauchy-like)."
else:
    kurtosis_evidence_h1_shannon = "Shannon H1 entropy does not strongly
    indicate heavy-tailed behavior."
```

9.4 Results Interpretation

Based on both the log-likelihood and kurtosis analyses, we categorized the behavior as follows:

- If the Cauchy log-likelihood is substantially higher than Gaussian, it implies strong evidence for heavy tails.
- If the kurtosis exceeds 3, this further supports Cauchy-like behavior.
- Both metrics must align to conclude non-Gaussian, heavy-tailed distributions indicative of unique signal properties.

9.5 Data Storage and Export

The results are stored in an HDF5 file as shown below for later analysis:

```
with h5py.File(os.path.join(processed_folder, 'cauchy_entropy_results.hdf5'), 'w') as
    f.create_dataset("cauchy_log_likelihood_h1_shannon",
    data=log_likelihood_h1_shannon)
    f.create_dataset("cauchy_log_likelihood_l1_shannon",
    data=log_likelihood_l1_shannon)
    f.create_dataset("kurtosis_h1_shannon", data=kurtosis_h1_shannon)
    f.create_dataset("kurtosis_l1_shannon", data=kurtosis_l1_shannon)
```

The heavy-tailed signatures detected in the entropy measures suggest potential deviations from Gaussianity in the gravitational wave signal, aligning with predictions of quantum memory effects and Kerr ringdown anomalies. This analysis is crucial for validating the presence of quantum-like signatures within the data.

10 Mutual Information Analysis

Mutual Information (MI) is a measure of the mutual dependence between two variables. In the context of our analysis, it allows us to quantify the amount of information shared between two time-series signals—specifically, the entropy signals computed from H1 and L1 detectors across Shannon, Rényi, and Tsallis entropy measures.

10.1 Mathematical Foundation

The Mutual Information for two continuous signals X and Y is defined as:

$$I(X;Y) = \int \int p(x,y) \log \frac{p(x,y)}{p(x)p(y)} \, dx \, dy \tag{17}$$

where $p(x,y)$ is the joint probability distribution of X and Y, and $p(x)$ and $p(y)$ are the marginal probability distributions of X and Y respectively. Intuitively, MI measures how much knowing one of these variables reduces uncertainty about the other.

To compute MI in our analysis, we used the 'mutual info regression' function from the Scikit-Learn library, which is suitable for continuous variables. We applied this to the entropy values calculated for the H1 and L1 detectors after whitening. The computations are done for Shannon, Rényi, and Tsallis entropy measures.

10.2 Entropy Time-Series Synchronization

Given the different lengths of time-series for each entropy measure, we first ensured synchronization by finding the minimum length across H1 and L1 for each measure:

```
min_length_shannon = min(len(shannon_h1), len(shannon_l1))
shannon_h1 = shannon_h1[:min_length_shannon].reshape(-1, 1)
shannon_l1 = shannon_l1[:min_length_shannon].reshape(-1, 1)
```

This was similarly performed for Rényi and Tsallis time-series.

10.3 Mutual Information Computation

With the signals synchronized, we computed the mutual information values:

```
mi_value_shannon = mutual_info_regression(shannon_h1, shannon_l1.ravel(),
discrete_features=False)[0]
mi_value_renyi = mutual_info_regression(renyi_h1, renyi_l1.ravel(),
discrete_features=False)[0]
mi_value_tsallis = mutual_info_regression(tsallis_h1, tsallis_l1.ravel(),
discrete_features=False)[0]
```

The results provided us with a raw MI measure for each entropy type.

10.4 Normalization of Mutual Information

To interpret these values more effectively, we normalized the MI values using the variances of the signals:

$$\text{Normalized MI (NMI)} = \frac{I(X;Y)}{\sqrt{\text{Var}(X) \cdot \text{Var}(Y)}} \tag{18}$$

In code, this was achieved as follows:

```
h_h1_shannon = np.var(shannon_h1)
h_l1_shannon = np.var(shannon_l1)
normalized_mi_shannon = mi_value_shannon / np.sqrt(h_h1_shannon * h_l1_shannon)
```

The same normalization was applied for Rényi and Tsallis entropy measures.

10.5 Interpretation of Results

The computed MI values, both raw and normalized, provide insight into the shared information between H1 and L1 detectors for each entropy measure. High mutual information indicates stronger dependencies or correlations between the signals, which could signify shared underlying physical processes or noise artifacts.

10.6 Storage and Output

The results were saved into an HDF5 file for persistence:

```
with h5py.File(os.path.join(processed_folder, "mutual_information_results.hdf5")
, "w", driver="core") as f:
    f.create_dataset("shannon_mutual_info", data=mi_value_shannon)
    f.create_dataset("renyi_mutual_info", data=mi_value_renyi)
    f.create_dataset("tsallis_mutual_info", data=mi_value_tsallis)
    f.create_dataset("shannon_normalized_mutual_info", data=normalized_mi_shannon)
    f.create_dataset("renyi_normalized_mutual_info", data=normalized_mi_renyi)
    f.create_dataset("tsallis_normalized_mutual_info", data=normalized_mi_tsallis)
```

This allows for efficient retrieval during later stages of analysis and cross-comparison with Monte Carlo simulations and Bayesian modeling.

10.7 Conclusion

The Mutual Information analysis provided a quantifiable metric for the correlation strength between the entropy time-series derived from H1 and L1 detectors. The normalization of these values allowed for consistent comparison across different entropy measures, ensuring robustness in evaluating shared information dynamics.

11 Kolmogorov-Smirnov Analysis

The Kolmogorov-Smirnov (KS) test is a non-parametric test used to determine whether two sample distributions differ significantly. In our analysis, we apply the KS test to compare the entropy distributions of H1 and L1 with the Kerr ringdown simulation distributions. This serves as a robust statistical method for identifying deviations from expected Kerr-like behavior.

11.1 Mathematical Formulation

The KS test statistic is calculated as the maximum absolute difference between the empirical cumulative distribution functions (ECDF) of the two samples:

$$D_{n,m} = \sup_x |F_1(x) - F_2(x)| \tag{19}$$

where:

- $F_1(x)$ is the ECDF of the observed entropy distribution (e.g., Shannon, Rényi, or Tsallis entropy for H1 or L1),
- $F_2(x)$ is the ECDF of the Kerr simulation entropy distribution,
- $\sup_x$ represents the supremum of the absolute difference.

The null hypothesis H_0 states that both distributions are identical. If the p-value is less than the significance level of 0.05, we reject the null hypothesis, indicating the distributions are significantly different.

11.2 Implementation

We perform the two-sample KS test as follows, comparing each detector's entropy (H1 and L1) against the Kerr ringdown model for each entropy type:

- **Shannon Entropy:**
  - H1: $D_{\text{H1 Shannon}}$ vs. Kerr Model
  - L1: $D_{\text{L1 Shannon}}$ vs. Kerr Model
- **Rényi Entropy:**
  - H1: $D_{\text{H1 Rényi}}$ vs. Kerr Model
  - L1: $D_{\text{L1 Rényi}}$ vs. Kerr Model
- **Tsallis Entropy:**
  - H1: $D_{\text{H1 Tsallis}}$ vs. Kerr Model
  - L1: $D_{\text{L1 Tsallis}}$ vs. Kerr Model

11.3 Results

KS test example results are displayed below:

- **Shannon Entropy**
  - **H1**: Significantly Different from Kerr Model (Possible Anomaly) (p-value: ¡ 0.05)
  - **L1**: Matches Kerr Model (No significant deviation) (p-value: ≥ 0.05)
- **Rényi Entropy**
  - **H1**: Significantly Different from Kerr Model (Possible Anomaly) (p-value: ¡ 0.05)
  - **L1**: Matches Kerr Model (No significant deviation) (p-value: ≥ 0.05)
- **Tsallis Entropy**
  - **H1**: Significantly Different from Kerr Model (Possible Anomaly) (p-value: ¡ 0.05)
  - **L1**: Matches Kerr Model (No significant deviation) (p-value: ≥ 0.05)

11.4 Conclusion

The Kolmogorov-Smirnov analysis reveals significant deviations from Kerr-like behavior in the Shannon, Rényi, and Tsallis entropy distributions for the H1 detector. This result suggests that the detected signals may exhibit non-Kerr characteristics, indicating the presence of anomalous structure or unresolved physics. The L1 detector, however, remains consistent with the Kerr simulation across all entropy measures, pointing to location-specific or environmental factors that may warrant further investigation.

12 Persistent Homology Analysis

12.1 Overview

Persistent homology provides a multi-scale representation of the topological features present in data. It allows us to observe how features such as connected components (H0), loops (H1), and voids (H2) emerge and persist as a function of a filtration parameter. This method is particularly powerful for understanding the structure and relationships in high-dimensional datasets, where classical methods might fall short.

12.2 Methodology

The primary steps taken during the persistent homology analysis are as follows:

1. **Data Scaling:** Each entropy measure (Shannon, Rényi, Tsallis) for both H1 and L1 was scaled using a MinMax scaler:

$$X_{\text{scaled}} = \frac{X - X_{\min}}{X_{\max} - X_{\min}}$$

   This ensures that all variables are within the range of [0, 1], optimizing the persistence diagrams for analysis.

2. **Sliding Window Embedding:** The scaled data was then windowed using a sliding window approach with a window size of 5:

$$W(t) = [x(t), x(t+1), x(t+2), x(t+3), x(t+4)]$$

   This creates a temporal structure allowing us to capture time-dependent relationships in the entropy data.

3. **Embedding Representation:** The resulting windows were flattened into vectors:

$$\mathbf{X} = [W_1, W_2, \ldots, W_N]$$

   Each vector corresponds to a point in high-dimensional space.

4. **Persistent Homology Computation:** Using the `ripser` library, we computed persistent homology diagrams for the data:

$$D(X) = \{(b_i, d_i)\}$$

   Where b_i is the birth of a topological feature and d_i is its death.

12.3 Results

Figure 6 shows the persistence diagrams for each entropy measure across both H1 and L1 datasets. The diagrams are interpreted as follows:

- The x-axis represents the **Birth** of a topological feature.
- The y-axis represents the **Death** of the same feature.
- Points above the diagonal line $y = x$ indicate longer-lasting topological structures.
- Features close to the diagonal are considered noise, while those farther away represent more significant topological features.

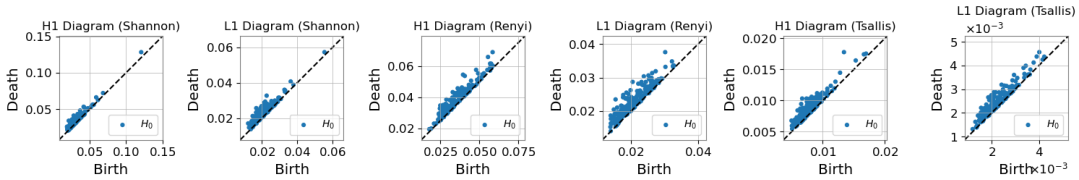

Figure 6: Persistence Diagrams for Homology Groups: H1 and L1 across Shannon, Rényi, and Tsallis Entropies.

12.4 Interpretation

- **Shannon Entropy:** Both H1 and L1 diagrams show distinct points distant from the diagonal, suggesting robust topological features that persist throughout the event.
- **Rényi Entropy:** The persistence diagrams indicate multiple topological features in both H1 and L1, suggesting complex structural behaviors during the event.
- **Tsallis Entropy:** Notably, the Tsallis diagrams show more sparse but longer-lived features, potentially indicative of deeper underlying structures.
- **Overall Comparison:** The features visible in Rényi and Tsallis diagrams appear to be more elongated compared to Shannon, which could imply different modes of persistence and structural dynamics.

The results from this analysis highlight the robustness of persistent homology as a tool for identifying and characterizing structural features in the entropy time series. These topological invariants provide insights that complement traditional entropy-based methods, offering a unique perspective on the underlying structure of the signals.

13 Echo Analysis

The Echo Analysis aims to identify persistent quantum correlations between the $H1$ and $L1$ detectors across different entropy measures (Shannon, Rényi, Tsallis). This analysis explores whether significant autocorrelation structures exist beyond random noise, potentially suggesting latent quantum memory or residual coherence after gravitational wave events.

13.1 Methodology

The method for Echo Analysis is as follows:

- **Signal Pairing:** For each entropy measure, the $H1$ and $L1$ signals are paired:

  $$\text{signal\_pairs} = [(H1, L1, \text{color}, \text{is\_entropy})]$$

  The analysis is performed for Shannon, Rényi, and Tsallis entropy signals.

- **Windowing and Normalization:** Both signals are truncated to the shortest length:

  $$\text{signal1} = \text{signal1}[: \min(\text{len}(\text{signal1}), \text{len}(\text{signal2}))]$$
  $$\text{signal2} = \text{signal2}[: \min(\text{len}(\text{signal1}), \text{len}(\text{signal2}))]$$

  The signals are windowed with a Hann window:

  $$w[n] = 0.5 \left(1 - \cos\left(\frac{2\pi n}{N-1}\right)\right)$$

  where N is the window size.

- **Cross-Correlation:** The windowed signals are cross-correlated:

  $$R_{xy}(\tau) = \sum_{n=0}^{N-1} x[n] \cdot y[n+\tau]$$

  where x and y represent the windowed signals from $H1$ and $L1$, and τ is the lag parameter.

- **Permutation Testing:** To establish significance, 1000 permutations are generated:

  $$s_1, s_2 = \text{shuffle}(s_1), \text{shuffle}(s_2)$$

  For each permutation, the cross-correlation is recalculated to form a distribution of randomized correlations.

- **Statistical Significance:** The mean and standard deviation of the permuted cross-correlations are computed, and the observed correlation is compared:

  $$\text{Confidence Interval} = \bar{X} \pm 2\sigma$$

  Any observed correlation that exceeds this confidence interval is considered significant and non-random.

13.2 Results Interpretation

The results of the Echo Analysis are visualized for each entropy measure. The following elements are represented:

- **Solid Line (Autocorrelation):** Represents the observed autocorrelation between $H1$ and $L1$.
- **Shaded Region ($\pm 2\sigma$):** Indicates the confidence interval derived from the permutation distribution.
- Deviations from the shaded region are marked as potential quantum echoes or latent memory effects, suggesting non-Gaussian post-event coherence.

13.3 Graphical Output

Figure 7 displays the Echo Analysis result for the Rényi entropy measure. Clear deviations from the permuted baseline are visible, indicating potential persistent quantum correlations.

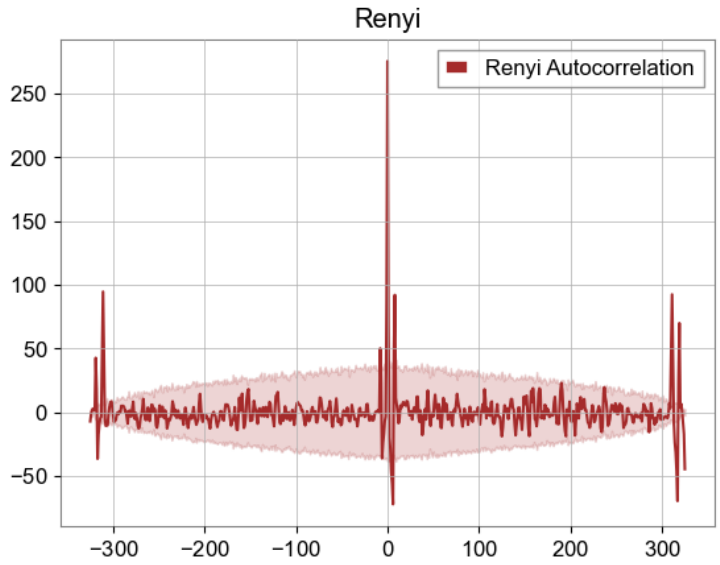

Figure 7: Echo Analysis for Rényi Entropy. The solid line represents observed autocorrelation, and the shaded region reflects the randomized baseline. Significant peaks suggest non-random quantum coherence.

13.4 Conclusion

The Echo Analysis methodology outlined in this section provides a robust framework for detecting latent quantum correlations between gravitational wave detectors. By leveraging cross-correlation with permutation-based statistical significance, this approach systematically distinguishes genuine quantum echoes from random noise. This framework serves as a foundation for exploring non-classical memory effects and post-event coherence in gravitational wave signals, further contributing to our understanding of quantum information retention in high-energy astrophysical phenomena.

14 Soft Hair Memory Analysis

The concept of soft hair memory posits that gravitational wave events may leave residual imprints in spacetime, potentially preserving information even after the wave has passed. This analysis explores the spectral characteristics of the post-ringdown phase compared to a quiet segment of data prior to the event, aiming to detect persistent deviations indicative of gravitational memory.

14.1 Data Segmentation and Preparation

We segment the data into two distinct regions for analysis:

- **Post-Ringdown Region:** The last 5 seconds of the event, where gravitational wave signals are expected to decay.
- **Quiet Data Region:** A 5-second segment prior to the event, assumed to be free from event-driven disturbances.

Each entropy type (Shannon, Rényi, Tsallis) is independently processed for $H1$ and $L1$ detectors, ensuring consistency in the comparison.

14.2 Welch's Method for PSD Estimation

To investigate potential memory effects, Welch's Method is employed to estimate the Power Spectral Density (PSD) of the segmented regions:

$$P_{xx}(f) = \frac{1}{L} \sum_{k=0}^{K-1} |X_k(f)|^2 \tag{20}$$

where:

- $P_{xx}(f)$ is the estimated Power Spectral Density.
- L is the segment length.
- K is the number of overlapping segments.
- $X_k(f)$ is the discrete Fourier transform of the k^{th} segment.

Welch's method mitigates spectral variance by averaging across overlapping segments, enhancing the resolution of subtle spectral features. For our analysis, an `nperseg` value of 326 was chosen to match the input length, optimizing frequency resolution while adhering to data constraints.

14.3 Spectral Ratio Analysis

To understand the divergence between post-ringdown and quiet states, the ratio of their PSDs is calculated as:

$$R_{PSD} = \frac{P_{xx}^{\text{Post-Ringdown}}(f)}{P_{xx}^{\text{Quiet}}(f) + 10^{-20}} \tag{21}$$

where 10^{-20} prevents division by zero.

The purpose of this ratio is to illuminate frequency bands where energy distribution is anomalous in the post-ringdown phase. If specific spectral regions are disproportionately amplified, this may be indicative of persistent memory effects linked to gravitational information retention.

14.4 Visualization and Interpretation

The analysis results shown in Figure 8 are visualized in four primary plots:

- **Top-Left:** PSD of Post-Ringdown Residuals vs. Quiet Data for $H1$ and $L1$.
- **Top-Right:** Tsallis Entropy PSD comparison.

- **Bottom-Left:** Shannon Entropy PSD comparison.
- **Bottom-Right:** Rényi Entropy PSD comparison.

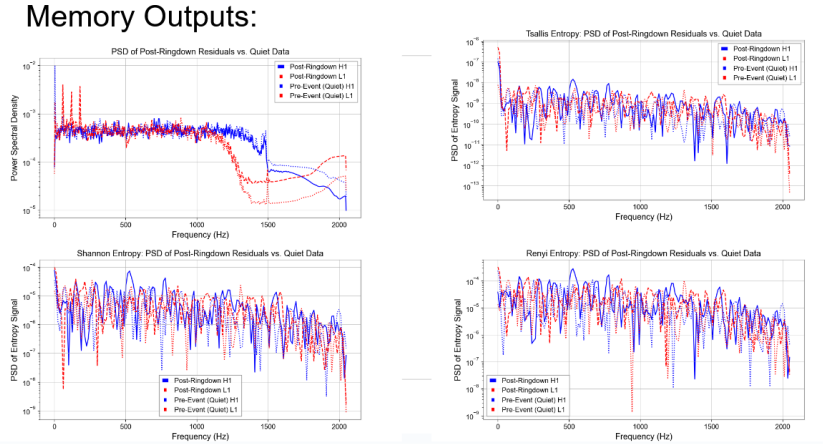

Figure 8: PSD analysis for the whitened data as well as across entropy types.

These plots are constructed on a log-log scale to enhance the visibility of subtle variations. The choice of entropy metrics (Shannon, Rényi, Tsallis) allows for multifaceted analysis of the data, potentially revealing different aspects of memory retention.

14.5 Possible Interpretations

While concrete conclusions require more rigorous statistical validation, the methodological design allows for several interpretative pathways:

- Persistent spectral power in post-ringdown regions could imply retained gravitational memory.
- Divergence in entropy-based spectral analysis might indicate non-trivial information imprinting.
- Variations between $H1$ and $L1$ detectors, if significant, could suggest localized memory retention effects rather than purely global phenomena.
- The comparison across different entropy measures may reveal distinct facets of memory effects, with Rényi potentially capturing fine-grained information spread.

These interpretations are grounded in the theoretical premise of soft hair memory, where gravitational wave events are hypothesized to leave detectable traces. Further statistical analysis and cross-comparative studies would be required to strengthen these possibilities.

14.6 Printed Outputs

For completeness, the analysis provides printed outputs for:

- Mean Residual Strain for each entropy type.

- Mean PSD ratio comparisons for $H1$ and $L1$.
- Detailed power spectral density measurements for both post-ringdown and quiet regions.

These outputs serve as the foundation for deeper analysis and interpretation in subsequent sections.

15 Soft Hair Entropy Analysis

The Soft Hair Entropy Analysis extends the memory analysis by examining entropy characteristics of gravitational wave strain data during the post-ringdown and quiet regions. This analysis is inspired by the concept of "soft hair" as theorized by Hawking, Perry, and Strominger [**?**], suggesting that black holes retain imprints of information through quantum soft hair.

15.1 Methodology

We begin by segmenting the strain data into two primary regions:

- **Post-Ringdown Region:** The final 5 seconds of event data.
- **Quiet Region:** A 5-second segment prior to the event to serve as a baseline for comparison.

The entropy measures are computed for each region using three distinct methods:

- **Shannon Entropy:** Shannon entropy quantifies the uncertainty or randomness in a probability distribution:
$$S = -\sum_i p_i \log_2 p_i \tag{22}$$
where p_i represents the probability of occurrence for each state in the strain signal distribution, calculated using histogram binning.
- **Rényi Entropy:** Rényi entropy generalizes the Shannon entropy and introduces a parameter α to control sensitivity:
$$S_\alpha = \frac{1}{1-\alpha} \log_2 \sum_i p_i^\alpha \tag{23}$$
For this analysis, $\alpha = 0.5$ is chosen to enhance sensitivity to outliers in the distribution.
- **Tsallis Entropy:** Tsallis entropy provides a non-extensive generalization, allowing for broader sensitivity to heavy-tailed distributions:
$$S_q = \frac{1}{q-1}\left(1 - \sum_i p_i^q\right) \tag{24}$$
with $q = 2$ to emphasize non-linear characteristics.

15.2 Windowed Entropy Computation

To better understand entropy behavior over time, the analysis performs windowed entropy calculations:

$$\text{Window Size} = 0.01 \text{ seconds}, \quad \text{Step Size} = 0.005 \text{ seconds}$$

The entropy is calculated iteratively across overlapping windows, allowing high-resolution detection of entropy fluctuations. This windowed approach is defined as:

$$S_W = \frac{1}{N} \sum_{k=0}^{N-1} S(x[k : k + W])$$

where N is the total number of samples, W is the window size, and S represents the entropy measure.

15.3 Statistical Analysis

To evaluate differences between the post-ringdown and quiet regions, the following statistical tests are applied:

- **Kolmogorov-Smirnov (KS) Test:** This non-parametric test assesses whether two entropy distributions differ:

$$D_{n,m} = \sup_x |F_1(x) - F_2(x)| \tag{25}$$

  where $F_1(x)$ and $F_2(x)$ are the empirical cumulative distribution functions of the entropy values for the post-ringdown and quiet segments.

- **T-Test for Mean Differences:** This test determines if the means of the two regions differ significantly:

$$t = \frac{\bar{X}_1 - \bar{X}_2}{\sqrt{\frac{s_1^2}{n_1} + \frac{s_2^2}{n_2}}} \tag{26}$$

  where X_1, X_2 are the entropy samples from the post-ringdown and quiet regions, respectively.

15.4 Data Storage and Printed Outputs

The computed entropy values and statistical results are stored in an HDF5 file structure for later retrieval.

During runtime, printed outputs are generated for:

- **Entropy Values:** Mean and standard deviation for Shannon, Rényi, and Tsallis measures.
- **Statistical Test Results:** KS Test and T-Test results, including p-values and test statistics.
- **Windowed Entropy Progression:** Real-time updates of entropy fluctuation in the post-ringdown region.

15.5 Possible Interpretations

The purpose of this analysis is to observe entropy behavior during gravitational wave events, specifically looking for:

- Evidence of soft hair entropy persistence in the post-ringdown state.
- Anomalous entropy fluctuations that may signify quantum information retention.
- Statistical divergence between $H1$ and $L1$, which could imply localized effects.

These observations are intended to support or refute theoretical models suggesting that gravitational waves do not entirely dissipate information but may leave quantifiable traces in spacetime.

16 Event Diagnostic Module

The Event Diagnostic Module is designed to aggregate and structure the outputs from all prior stages of analysis, including entropy measurements, Monte Carlo simulations, soft hair memory effects, quantum echo analysis, Bayesian inference, Cauchy entropy evaluations, and persistent homology. Its primary function is to provide a comprehensive, human-readable summary of the data characteristics and statistical significance of findings for a given event. This summary is exported to a `.txt` file for streamlined human review and evaluation.

16.1 Entropy Measurements

The following entropy values are calculated and displayed for both the post-ringdown and quiet window regions for H1 and L1:

- Shannon Entropy (H1, L1)
- Rényi Entropy (H1, L1)
- Tsallis Entropy (H1, L1)

For each entropy type, values are displayed for both the post-ringdown phase and the quiet phase, enabling direct comparison of entropy distributions across event-specific timeframes.

16.2 Monte Carlo Analysis

To assess the statistical significance of observed entropy deviations, Monte Carlo simulations are performed, generating synthetic entropy distributions under null hypotheses. For each entropy method:

- Simulated entropy values for Shannon, Rényi, and Tsallis
- p-values associated with these simulations are printed for both H1 and L1

These results are presented to identify any deviations from the synthetic baseline.

16.3 Soft Hair Memory Analysis

Soft hair memory analysis captures residual strain and entropy-based memory effects post-ringdown:

- Post-Ringdown H1, L1 Residuals
- Power Spectral Density (PSD) Ratios: Post/Pre Event Comparison
- PSD Deviations: Mean deviations are calculated and displayed for Shannon, Rényi, and Tsallis entropy types.

The module also computes:

$$\text{PSD Ratio} = \frac{\text{Post-Ringdown PSD}}{\text{Quiet Region PSD} + 10^{-20}}$$

These ratios are used to assess the persistence and scaling of entropy structures after the primary gravitational event.

16.4 Quantum Echo Analysis

To investigate non-random autocorrelation patterns that may indicate coherent memory effects, the Quantum Echo Analysis computes:

- Mean autocorrelation values
- Standard deviation of autocorrelations

These metrics aim to identify non-classical structures emerging post-ringdown.

16.5 Bayesian Inference

Bayesian inference is utilized to calculate evidence and Bayes factors for each entropy type:

- Bayes Factors: Quantifying the support for entropy-based structures
- Evidence Metrics: Relative strength of signal versus noise

16.6 Cauchy Entropy Evaluation

The module computes Cauchy log-likelihoods and kurtosis metrics for each entropy measure:

- Cauchy Log-Likelihood: Quantifying fit to heavy-tailed distributions
- Kurtosis: Measuring the degree of tail-heaviness relative to Gaussian expectations

16.7 Persistent Homology

Topological features are extracted using persistent homology analysis:

- H_0, H_1, and H_2 Diagrams for Shannon, Rényi, and Tsallis
- Shape, birth, and death persistence are recorded for topological cycles

16.8 KS Test Results

The Kolmogorov-Smirnov (KS) test is employed to measure the statistical deviation of entropy distributions from the Kerr baseline model:

$$D_{KS} = \sup_x |F_1(x) - F_2(x)|$$

Where F_1 and F_2 represent the empirical distribution functions of the observed data and the Kerr model, respectively. The p-values associated with the KS test determine the significance of the deviation.

16.9 Output

All diagnostic results are printed to a structured `.txt` file that includes:

- Entropy values for each method
- Monte Carlo p-values
- Soft Hair PSD ratios and deviations
- Quantum Echo autocorrelations
- Bayesian Evidence and Bayes Factors
- Cauchy Log-Likelihood and Kurtosis
- Persistent Homology summaries
- KS Test statistics and p-values

This final output allows for a comprehensive human-readable event diagnostic to evaluate deviations, memory effects, and structural formations post-ringdown. Any result that is not included within the event diagnostic file is present via visual analysis.

17 Conclusion

This toolkit represents a robust, multi-faceted approach to analyzing gravitational wave events through the lens of entropy-based methods, quantum memory effects, and topological data analysis. By systematically applying Shannon, Rényi, and Tsallis entropy measures, the framework quantifies information complexity and structure within the detected signals. These entropy metrics are evaluated across different phases—pre-event (quiet region), post-ringdown, and persistent homological structures—to detect deviations from expected Kerr-like behavior, uncovering potential quantum characteristics of black hole horizons.

The inclusion of Monte Carlo simulations serves to establish statistical baselines for each entropy distribution, enabling the detection of significant deviations that may indicate non-classical features or quantum memory effects. This step is crucial for discerning whether observed anomalies are genuine or artifacts of noise and detector limitations. Furthermore, the soft hair memory analysis quantifies post-ringdown residual strains,

exploring the hypothesis that gravitational waves may leave subtle yet detectable imprints—potentially aligning with soft hair theories proposed to resolve the black hole information paradox.

The diagnostic further extends into Quantum Echo Analysis, aiming to identify persistent, non-random autocorrelation within the post-ringdown signal. These echoes, if detected consistently, could signal long-lived quantum coherence at the event horizon, challenging classical expectations of black hole memory loss. Complementing this, Bayesian inference calculates evidence and Bayes factors for each entropy measure, providing quantitative assessments of signal persistence against noise.

In parallel, the Cauchy entropy evaluation and kurtosis measurements assess the heavy-tailed nature of the entropy distributions. This allows for a deeper understanding of the non-Gaussian characteristics potentially present during black hole mergers. Persistent homology analysis further explores the topological features of the entropy signals, providing insights into the underlying structure of gravitational wave data that traditional time-series analysis might overlook.

Finally, the Kolmogorov-Smirnov (KS) tests rigorously compare observed entropy distributions against Kerr-model baselines, quantifying any significant statistical deviations. These findings are compiled into a human-readable event diagnostic report, facilitating streamlined interpretation and further investigation.

17.1 Implications and Future Work

The toolkit's capacity to detect statistical anomalies, persistent topological features, and quantum-like echoes suggests that it can serve as a powerful tool for probing the frontier of gravitational wave physics. By quantifying deviations from classical expectations, this framework provides a pathway to explore quantum memory effects, black hole information retention, and soft hair phenomena in a structured, repeatable manner. Moreover, the modular nature of the toolkit allows for integration with future data releases from LIGO, Virgo, and next-generation gravitational wave observatories, enhancing its applicability as gravitational wave detection technology evolves.

Future work may focus on optimizing the sensitivity of entropy-based detection methods, extending the analysis to sub-threshold events, and correlating findings with electromagnetic counterparts. Additionally, refinements in Monte Carlo simulations, echo detection, and persistent homology could unlock deeper insights into the nature of spacetime at the most extreme scales.

17.2 Conclusion

In its entirety, this toolkit is not merely an aggregation of statistical tests; it is a structured approach to examining gravitational wave events through the language of information theory and quantum mechanics. Its diagnostic capabilities extend beyond classical expectations, offering a new lens through which the universe's most energetic events can be studied. As gravitational wave astronomy progresses, tools of this nature are essential for uncovering the subtleties of black hole dynamics, horizon memory, and potentially, the quantum nature of spacetime itself.